

Mode-coupling theory of the fifth-order Raman spectrum of an atomic liquid

R. Aldrin Denny and David R. Reichman

Harvard University, 12 Oxford Street, Cambridge, Massachusetts 02138

(Received 2 December 2000; published 10 May 2001)

A fully microscopic molecular hydrodynamic theory for the two-dimensional (fifth-order) Raman spectrum of an atomic liquid (Xe) is presented. The spectrum is obtained from a simple mode-coupling theory by projecting the dynamics onto bilinear pairs of fluctuating density variables. Good agreement is obtained in comparison with recently reported molecular dynamics simulation results. The microscopic theory provides an understanding of the timescales and molecular motions that govern the two-dimensional signal. Predictions are made for the behavior of the spectrum as a function of temperature and density. The theory shows that novel signatures in the two-dimensional Raman spectrum of supercritical and supercooled liquids are expected.

DOI: 10.1103/PhysRevE.63.065101

PACS number(s): 05.20.-y, 61.20.Lc, 78.30.Cp, 78.47.+p

Nonresonant nonlinear Raman spectroscopy holds the promise of providing crucial information concerning the coupling and dynamics of microscopic collective modes in condensed phase systems. In particular, fifth-order Raman spectroscopy has been proposed, in analogy to two-dimensional (2D) NMR, as a sensitive means to elucidate the mechanisms and timescales that govern the intricate motions that occur in complex liquids, polymeric systems, and proteins [1–5]. The important feature of this technique is its ability to differentiate between inhomogeneous and homogeneous broadening through the appearance or absence of an echo in the fifth-order signal.

Two obstacles have emerged in the pursuit of this goal. The first hurdle concerns the experimental detection of the spectrum. Early attempts to detect the fifth-order signal in liquids were contaminated by competing parallel cascade processes which masked the detection of the desired response profile [6]. Recently, however, several research groups have overcome this problem, and have detected fifth-order signals uncontaminated by cascades [7–9]. Difficulties have also appeared on the theoretical side. At present, the only fully microscopic theoretical calculation of the fifth-order Raman spectrum in a simple system (liquid Xe) predicts a strong echo, at variance with concurrent molecular dynamics simulations [10].

Given the fact that fifth-order Raman spectroscopy may indeed provide a powerful technique for the elucidation of collective motion in *complex* systems, it is of primary importance to develop a microscopic predictive theory of the fifth-order Raman signal in *simple* systems, such as atomic liquids. Not only would such a theory act as a foundation for the study of more complex systems, but it would also provide an understanding of exactly what the signal reveals with regard to the fundamental *intermolecular* dynamics of liquids. Here, we attempt to provide such a theory for the fifth-order Raman spectrum of liquid Xe [10].

We assume that Xe atoms interact via a Lennard-Jones potential and that the polarizability tensor of the sample is of the form

$$\Pi = \sum_{i=1}^N \alpha_i + \sum_{i \neq j}^N \alpha_i \cdot \mathbf{T}(\hat{r}_{ij}) \cdot \alpha_j, \quad (1)$$

where N is the number of atoms in the sample, α_i represents isolated polarizability tensor of atom i , $\mathbf{T}(\hat{r}_{ij})$ denotes the dipole-dipole interaction tensor between atoms i and j , and the notation \hat{A} is used as a reminder of the operator nature of the quantity under investigation. It should be noted that more realistic forms of the polarizability tensor are easily accommodated in our theory. The off-resonant fifth-order response function is expressed in terms of Heisenberg operators of the polarizability tensor at different times [3,4],

$$R^{(5)}(t_1, t_2) = \left(\frac{i}{\hbar} \right)^2 \langle [[\Pi(t_1 + t_2), \Pi(t_1)], \Pi(0)] \rangle, \quad (2)$$

where square brackets represent the commutator, i.e., $[A, B] = AB - BA$, and angular brackets indicate an ensemble (quantum) average over the initial conditions. Note that Π is a quantum mechanical operator, and that in any comparison with classical simulations, the classical limit must be taken carefully.

The only portion of the polarizability tensor that affects the time dependence of $R^{(5)}(t_1, t_2)$ is that containing $\mathbf{T}(\hat{r}_{ij})$. Note that $\mathbf{T}(\hat{r}_{ij})$ may be expressed in terms of density operators as

$$\sum_{i \neq j} \mathbf{T}^{\alpha\beta}(\hat{r}_{ij}) = \sum_{\mathbf{k}} \mathbf{T}_{\mathbf{k}}^{\alpha\beta}(\hat{\rho}_{-\mathbf{k}} \hat{\rho}_{\mathbf{k}} - N), \quad (3)$$

where $\mathbf{T}_{\mathbf{k}}^{\alpha\beta}$ is the wave-vector Fourier transform of the $\alpha\beta$ component of the dipole-dipole interaction tensor and the density operator $\hat{\rho}_{\mathbf{k}}$ is given by $\hat{\rho}_{\mathbf{k}} = \sum_{i=1}^N \exp(i\mathbf{k} \cdot \hat{\mathbf{r}}_i)$. Due to the fact that, *for all times*, the dynamically important piece of Π may be decomposed into fluctuating pairs of density operators, a simple mode-coupling approach is suggested [11–14]. In this approach, the dynamically relevant portion of the polarizability tensor is projected onto bilinear pairs of fluctuating density operators. In particular, we replace \mathbf{T} with its projection onto fluctuating bilinear pairs of density operators as $\mathbf{T} \rightarrow \wp \mathbf{T}$, where

$$\wp \hat{A} = \lim_{q \rightarrow 0} \frac{1}{2N^2} \sum_{\mathbf{k}} \frac{\hat{R}_{\mathbf{k}, \mathbf{q}-\mathbf{k}}}{S_Q(k) S_Q(|q-k|)} \langle \hat{R}_{\mathbf{k}, \mathbf{q}-\mathbf{k}}^\dagger \hat{A} \rangle, \quad (4)$$

$\hat{R}_{\mathbf{k},\mathbf{q}-\mathbf{k}} = \hat{\rho}_{\mathbf{k}}\hat{\rho}_{\mathbf{q}-\mathbf{k}}$, $S_Q(k)$ is the (quantum) static structure factor at wave vector k [$S_Q(k) = \langle \hat{\rho}_{-\mathbf{k}}\hat{\rho}_{\mathbf{k}} \rangle / N$], and \hat{A} is an arbitrary quantum operator that depends only on nuclear position. Note that the projection operator \wp is simply the zero wave-vector limit of a quantum version of the projector used to derive the mode-coupling equations for the dynamic structure factor [15]. The subscript ‘‘Q’’ is used to remind the reader that the quantity in question is calculated via a quantum mechanical averaging procedure. The classical analogs of such quantities will appear without this subscript.

The fully quantum mechanical expression in Eq. (2) involves two commutators, and thus four distinct correlation functions, each consisting of the product of six density operators at different times, is obtained after $\mathbf{T}_{\alpha\beta}$ is replaced by its projection onto a bilinear pair of density variables. In this work, we will focus for simplicity on the fully polarized ($\alpha = z$, $\beta = z$) case. In the spirit of the *simplified* mode-coupling theory [11,12], the multitime correlation function is *approximated* as a factorized product of density correlators [as is the denominator in Eq. (4)]. Since the fully quantum mechanical expression involves *operators* of the fluid density, the proper time ordering of paired density variables must be maintained. Performing the above procedure yields, for the fully polarized signal,

$$R_{zzzzzz}^{(5)}(t_1, t_2) = \left(\frac{i}{\hbar}\right)^2 \sum_{\mathbf{k}} \left(\frac{V_Q^{zz}(\mathbf{k})}{S_Q(k)^2}\right)^3 \times [F_Q(k, t_2) - F_Q(k, -t_2)] \times [F_Q(k, t_1 + t_2)F_Q(k, t_1) - F_Q(k, -t_1 - t_2)F_Q(k, -t_1)], \quad (5)$$

where $F_Q(k, t)$ is the quantum mechanical intermediate scattering function ($F_Q(k, t) = \langle \hat{\rho}_{-\mathbf{k}}(t)\hat{\rho}_{\mathbf{k}}(0) \rangle / N$), and the vertex $V_Q^{zz}(\mathbf{k})$ is defined as

$$V_Q^{zz}(\mathbf{k}) = \frac{1}{N} \sum_i^N \sum_{j \neq i}^N \sum_{l, m}^N \langle T_{zz}(\hat{r}_{ij}) \exp(-i\mathbf{k} \cdot \hat{\mathbf{r}}_{lm}) \rangle.$$

Since we will eventually take the classical limit, we consider here the high temperature situation where this average can be performed classically. The classical vertex contains two, three, and four body coupling terms. Taking the classical limit of the expression in Eq. (5) we obtain

$$R_{zzzzzz}^{(5)}(t_1, t_2) = \frac{1}{(k_B T)^2} \sum_{\mathbf{k}} \left(\frac{V_Q^{zz}(\mathbf{k})}{S(k)^2}\right)^3 \frac{dF(k, t_2)}{dt_2} \times \frac{d}{dt_1} [F(k, t_1 + t_2)F(k, t_1)]. \quad (6)$$

Equation (6) predicts that the fifth-order response for an atomic liquid is governed by a complex interplay of density fluctuations. Note that this expression has fully microscopic predictive power. Given simple structural information one may predict the density and temperature dependence of the spectrum. The response is predicted to have novel signatures

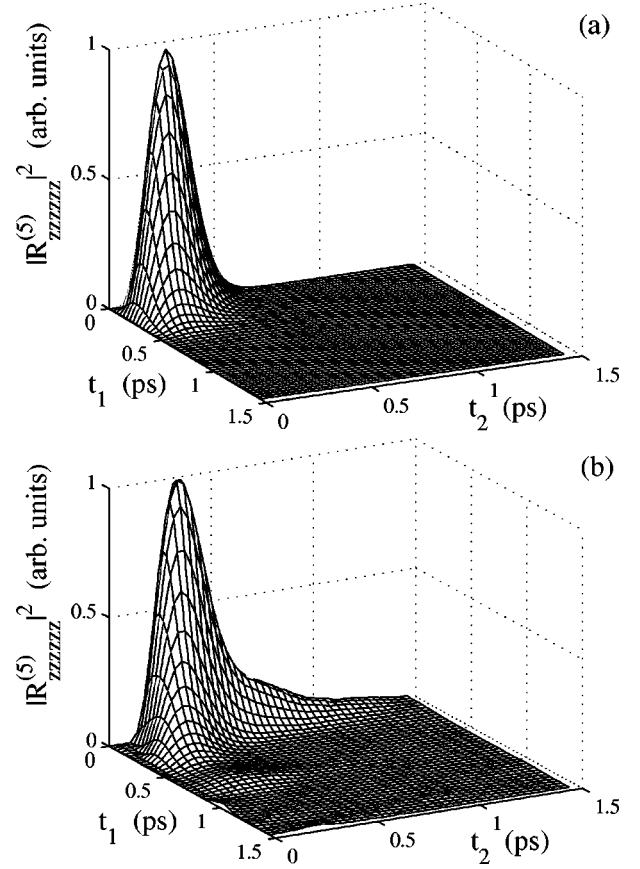


FIG. 1. Fifth-order Raman spectrum (fully polarized) obtained from theory (above) and simulation (below). The reduced density ρ^* and temperature T^* employed in the calculation are 0.8 and 1.0, respectively.

for liquids that are supercooled, where the tails of the signal develop a slow dynamical character. In particular, due to the multitime nature of the fifth-order response, and the underlying role of density fluctuations (in simple systems), our theory highlights the potential use of studying *dynamic heterogeneity* in supercooled liquids [16]. A more quantitative discussion of this connection will be given elsewhere [17]. Equation (6) also predicts interesting behavior near the liquid-gas critical point, where the correlation length for density fluctuations grows tremendously. A fully self-consistent calculation of the fifth-order Raman spectrum may be computed with a theory for the pair distribution function (giving a description of all structural input needed to compute the vertex within the generalized Kirkwood superposition approximation [17] and a (self-consistent) mode-coupling calculation of the density fluctuations [15]. Here, however, we explore the predictions of Eq. (6) by simulating the structural input and using the viscoelastic theory to generate the spectrum of density fluctuations [11].

The spectrum obtained from our theory is compared to the molecular dynamics (MD) simulation results of Ma and Stratt [10] in Figs. 1 and 2. The most striking feature of the spectra is the complete lack of an echo in the analytical result. This is precisely the behavior predicted by the simulation, but is described in a qualitatively improper fashion by

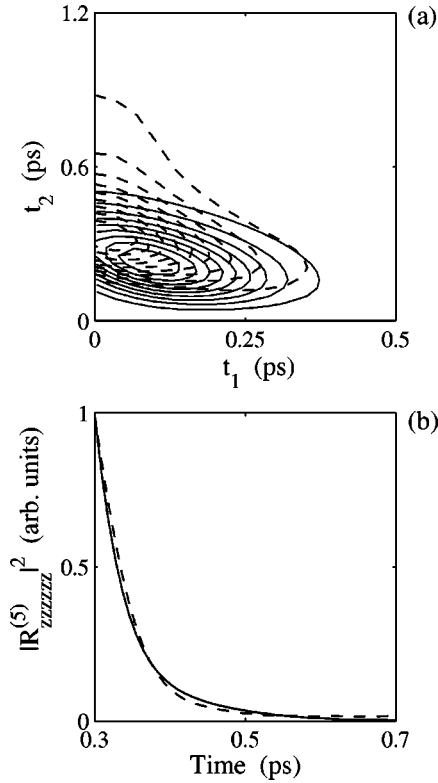


FIG. 2. Comparison of the mode coupling theory (solid line) results with MD simulation (dashed line) results for $\rho^* = 0.8$ and $T^* = 1.0$. (a) Contour plot of the fifth-order signal. (b) Normalized fully polarized signal along cut ($t_1 = t_2$) of the 2D spectrum.

the instantaneous normal mode calculation of Ma and Stratt [10]. Given the central role played by density fluctuations in our theory, the complete lack of an echo is not entirely surprising [18]. In general, the theory is in good agreement with the simulation results of Ma and Stratt. In particular, both the overall form of the signal, and the rotated, nearly ellipsoidal character of the response are well captured [19]. The mode-coupling theory presented here is expected to be more accurate at longer times. In Fig. 2(b) we compare the decay of the fifth-order response function under the condition $t_1 = t_2$ as computed by molecular dynamics simulation and Eq. (6). After approximately 200 fs the agreement is *quantitative*. One feature not captured is the “ridge” along the t_2 axis. This failing will be discussed before concluding.

The $R_{zzzzz}^{(5)}(t_1, t_2)$ signal observed is composed of contributions arising from different wave vectors, thus deciphering these contributions yields useful information concerning the various modes that are involved in the response. At high densities (for example $\rho^* > 0.8$), the contribution from the wave vectors $k\sigma < 4$, i.e., $r/\sigma > 1.57$ is around 20%, suggesting that the dynamics of the spectra are dominated by local (“first-shell”) events. For these high densities, higher wave vectors ($k\sigma > 10$) influence the response function greatly. However, for lower densities (i.e., $\rho^* = 0.8$), the contribution arising from $k\sigma < 4$ is more than 40% and longer wave vectors ($k\sigma > 10$) contribute only about 12%, suggesting that the distance between $r/\sigma \approx 0.8 - 2.0$ captures most of the dynamical information. Thus “second-shell” processes begin

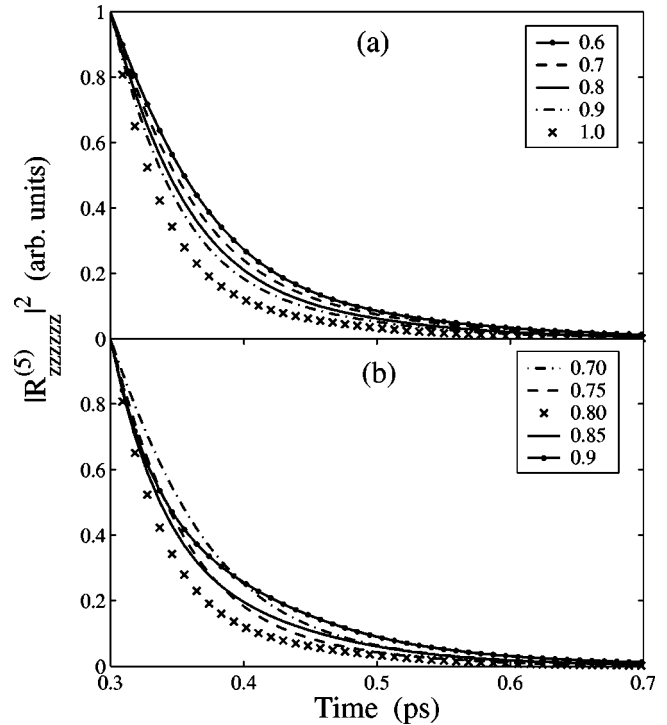


FIG. 3. Raman signal for various temperature (a) and density (b) values, along cut ($t_1 = t_2$) of the 2D spectrum. The normalized spectra are shown for $t \geq 300$ fs. Curves are for different (a) T^* ($\rho^* = 0.8$) and (b) ρ^* ($T^* = 1.0$) values.

to contribute nonnegligibly as well.

We now make predictions for the temperature and density dependence of the signal. We restrict our discussion to the dependence of the response on external parameters along the “echo direction” ($t_1 = t_2$). This is done for two reasons. First, the experimental interpretation of the signal should be most unambiguous along this direction. Second, the simple mode-coupling theory employed here will be most reliable outside the inertial regime, thus rendering the prediction of Eq. (6) most accurate away from the axes $t_1 = 0$ and $t_2 = 0$.

The temperature dependence of $|R_{zzzzz}^{(5)}(t_1, t_2)|^2$ for $t_1 = t_2$ is studied in Fig. 3(a). We monitor the decay of the signal after the strict inertial regime and normalize each curve for comparison. The decay curves show an increase in the rate of decay as the temperature is increased. This can be physically understood by the fact that a change in the temperature does not alter the static coupling parameters such as $S(k)$ and $V^{zz}(\mathbf{k})$ appreciably; however, at higher temperatures the dynamical quantity $F(k, t)$ decays noticeably faster due to the increased fluidity of the system.

An interesting feature of the decay along the echo direction is observed as the density of the liquid is varied. In Fig. 3(b) we plot the asymptotic decay of $|R_{zzzzz}^{(5)}(t_1, t_2)|^2$ for $t_1 = t_2$ as a function of density. Note that from $\rho^* = 0.7$ to $\rho^* = 0.8$ the decay of the fifth-order signal increases as a function of density increase. However, in the density range of $\rho^* = 0.8$ to $\rho^* = 0.9$ (the density of liquid-solid coexistence at $T^* = 1.0$) completely contrasting behavior is observed. For such higher densities, the (*normalized*) decay slows down. This can be understood as a type of de Gennes narrowing

[11]. As the dynamical phenomena become dominated by first-shell events, the dynamic structure factor exhibits a slowing down due to a sharp rise in the static structure factor for the wave vectors corresponding to localized, first-shell liquid structure.

Given the degree of complexity of the correlation function of Eq. (2) and the simplicity of Eq. (6), the results presented in Figs. 1 and 2 are rather remarkable. In particular, the off-axis response described by Eq. (6) is in quantitative agreement with simulation after ≈ 200 fs, where the amplitude of the signal is still experimentally detectable. This is significant, because it is this portion of the signal that will be most telling and interesting for the study of supercooled liquids [17,16]. However, there are limitations to the theoretical approach outlined here. We have used the term “simple” to describe the mode-coupling approach employed in this work. This is because the mode-coupling approximation has been performed directly on the desired correlation function, and not on an associated memory function [11,12]. Furthermore, the factorization of the multitime correlation function resulting in an expression that contains only the intermediate scattering function and no direct coupling between different wave vectors is expected to be less accurate in the strict short-time limit. The lack of a distinct ridge along the t_2 axis

as displayed by the simulation is probably a direct consequence of this shortcoming. Our treatment has not included corrections for inertial (binary) dynamical effects [20]. Note, however, that previous simple mode-coupling treatments that capture the correct initial value of the correlation function under study do indeed capture short-time effects reasonably well [11,13,14,21]. While those treatments use a wave-vector cutoff to enforce the proper initial value, the value $R^{(5)}(0,0)=0$ is automatically satisfied in the case of the fifth-order Raman signal due to the double commutator form of Eq. (2). It is thus expected that even the strict short-time behavior predicted by Eq. (6) will not be grossly inaccurate. In fact, our recent work on the simpler third-order signal strongly supports this claim [22]. It is hoped that future experiments on liquid Xe may indeed confirm the behavior displayed in Fig. 3. A demonstration of the predictive utility of the theory developed here for simple atomic systems may pave the way for an understanding of the microscopic contributions to the fifth-order Raman signal in more complex systems.

We thank Ao Ma for providing his simulation results, and Richard Stratton and Andrei Tokmakoff for helpful discussions.

-
- [1] S. Mukamel, A. Piryatinski, and V. Chernyak, *Acc. Chem. Res.* **32**, 145 (1999); Y. Tanimura and S. Mukamel, *J. Chem. Phys.* **99**, 9496 (1993).
- [2] T. Steffen, and K. Duppen, *J. Chem. Phys.* **106**, 3854 (1997); *Phys. Rev. Lett.* **76**, 1224 (1996).
- [3] K. Okumura and Y. Tanimura, *J. Chem. Phys.* **106**, 1687 (1997); **107**, 2267 (1997).
- [4] S. Saito and I. Ohmine, *J. Chem. Phys.* **108**, 240 (1998).
- [5] T. Keyes and J. T. Fourkas, *J. Chem. Phys.* **112**, 287 (2000); R. L. Murry, J. T. Fourkas, and T. Keyes, *ibid.* **109**, 7913 (1998).
- [6] D. A. Blank, L. J. Kaufman, and G. R. Fleming, *J. Chem. Phys.* **111**, 3105 (1999); D. J. Ulness, J. C. Kirkwood, and A. C. Albrecht, *ibid.* **108**, 3897 (1998).
- [7] D. A. Blank, L. J. Kaufman, and G. R. Fleming, *J. Chem. Phys.* **113**, 771 (2000).
- [8] V. Astinov, K. J. Kubarych, C. J. Milne, and R. J. D. Miller, *Chem. Phys. Lett.* **327**, 334 (2000).
- [9] O. Golonzka, N. Demirdöven, M. Khalil, and A. Tokmakoff, *J. Chem. Phys.* **113**, 9893 (2000).
- [10] A. Ma and R. M. Stratton, *Phys. Rev. Lett.* **85**, 1004 (2000).
- [11] U. Balucani and M. Zoppi, *Dynamics of The Liquid State* (Oxford University Press, New York, 1994); J.-P. Hansen and I. R. McDonald, *Theory of Simple Liquids*, 2nd ed. (Academic, London, 1990).
- [12] W. Götze and M. Lucke, *Phys. Rev. A* **11**, 2173 (1975).
- [13] T. Munakata and A. Igarashi, *Prog. Theor. Phys.* **60**, 45 (1978).
- [14] T. Geszti, *J. Phys. C* **16**, 5805 (1983).
- [15] W. Götze, in *Liquids, Freezing and the Glass Transition*, edited by J. P. Hansen, D. Levesque, and J. Zinn-Justin (North-Holland, Amsterdam, 1991), Vol. 1, Chap. 5, pp. 287–503.
- [16] See, for example, U. Tracht, M. Wilhelm, A. Heuer, H. Feng, K. Schmidt-Rohr, and H. W. Spiess, *Phys. Rev. Lett.* **81**, 2727 (1998); for a different measure of dynamic heterogeneity that does *not* involve multitime information, see S. C. Glotzer, V. N. Novikov, and T. B. Schröder, *J. Chem. Phys.* **112**, 509 (2000).
- [17] R. A. Denny and D. R. Reichman (unpublished).
- [18] M. Berg and D. A. Vanden Bout, *Acc. Chem. Res.* **30**, 65 (1997).
- [19] The recent studies of Blank *et al.* [7] and Golonzka *et al.* [9] also show that the off-axis signal has a rotated ellipsoidal character. This may be a general indication of the kind of translational motion discussed in this work.
- [20] K. Okumura, B. Bagchi, and Y. Tanimura, *Bull. Chem. Soc. Jpn.* **73**, 873 (2000).
- [21] U. Balucani, R. Vallauri, and T. Gaskell, *Phys. Rev. A* **35**, 4263 (1988).
- [22] R. A. Denny and D. R. Reichman (unpublished).